

# Adsorption of the Stable Radical Di-*tert*-butyl Nitroxide (DTBN) on an Epitaxially Grown Al<sub>2</sub>O<sub>3</sub> Film<sup>†</sup>

U. J. Katter, T. Hill, T. Risse, H. Schlien, M. Beckendorf, T. Klüner, H. Hamann, and H.-J. Freund\*

Lehrstuhl für Physikalische Chemie I, Ruhr-Universität Bochum, 44780 Bochum, Germany

Received: May 22, 1996; In Final Form: September 3, 1996<sup>⊗</sup>

The system di-*tert*-butyl nitroxide (DTBN) adsorbed on a thin film of  $\gamma$ -Al<sub>2</sub>O<sub>3</sub>(111) grown on a NiAl(110) single crystal has been studied with various surface science methods, including TPD, XPS, NEXAFS, and ESR line-shapes analysis. In the monolayer regime, two strong chemisorbed species with adsorption energies of 120 and 150 kJ/mol, respectively, are found after adsorption at 40 K. One species is ESR active and reveals distinct dynamic behavior above 200 K through cw ESR line-shape analysis. The second species is oriented with an angle of about 70° between the surface normal and the N–O axis of the molecule, as the NEXAFS data show. Missing of the  $\pi^*$  resonance and the ESR inactivity suggest a direct participation of the half-filled  $\pi^*$  orbital located at the nitrogen atom in the bonding mechanism. Above 200 K, both adsorbed species exchange with each other. This could be followed by monitoring the temperature-dependent ESR intensity. Adsorption at room temperature leads to the formation of a third unstable species which is ESR active but shows a different ESR spectrum in comparison with the other ESR-active species. The accessibility of the nitrogen atom for bonding is discussed on the basis of high-quality ab initio calculations.

## 1. Introduction

Surface science has been a growing field for longer than the last 3 decades.<sup>1</sup> A great variety of methods for the examination of well-ordered systems have been developed, in particular, various kinds of electron spectroscopies.<sup>2</sup> Both the properties of the clean surfaces themselves and the interaction between these surfaces and adsorbed molecules were accessed, also providing answers to questions concerning the properties of real catalysts.<sup>3</sup>

Unfortunately, there are only a few methods to directly study the dynamics on single-crystal surfaces<sup>4,5</sup> which can be fundamental in understanding catalytic processes. Molecules adsorb on a surface, diffuse, collide, and react. Translational diffusion may control this reaction, but rotational diffusion also contributes to the rate at which the molecules are oriented in a favorable way to react.

Nuclear magnetic resonance (NMR)<sup>6</sup> has been very helpful in the investigation of molecular motion in the liquid and solid phases as well as on powder samples.<sup>7</sup> But its limited sensitivity (10<sup>17</sup> nuclear spins necessary to obtain a reasonable signal-to-noise ratio) makes it impossible to utilize this method in surface science except in special cases.<sup>8</sup> In contrast, electron spin resonance (ESR)<sup>9</sup> needs less than 10<sup>13</sup> spins to detect an ESR signal under ambient conditions. So ESR has been established as a surface science tool in the last few years.<sup>10,11</sup> A disadvantage is the necessity for unpaired electrons to be present in the considered system, but if that is the case, the ESR spectrum may contain a large variety of information about the dynamics, orientation, concentration, and chemical environment of the adsorbed molecule. The combination of ESR spectroscopy with other surface science techniques will therefore lead to a much more complete description of these systems.

In this study, DTBN<sup>12</sup> has been adsorbed on a Al<sub>2</sub>O<sub>3</sub>(111) film, which is a model system for this important catalytic

surface.<sup>13</sup> DTBN and some other small nitroxide molecules have been used in several studies on polycrystalline powders to examine the reactions on the Al<sub>2</sub>O<sub>3</sub> surface<sup>14</sup> or its acidity.<sup>15</sup> Figure 1a shows the structure and size of the DTBN molecule, as given by a gas-phase electron diffraction study.<sup>16</sup> The unpaired electron, responsible for the radical character of the molecule, is located in an antibonding  $\pi^*$  orbital at the NO group, but the magnetic properties can be approximated by assuming that the unpaired electron occupies a p<sub>z</sub> orbital at the nitrogen atom.<sup>17</sup> The simplification is illustrated in Figure 1b, where the standard coordinate system for the nitroxide group is defined.

The information contained in the ESR spectra is filled out by the data gained with the other surface science techniques used here: NEXAFS (near-edge X-ray absorption fine structure), XPS (X-ray photoelectron spectroscopy), TPD (thermal programmed desorption), LEED (low-energy electron diffraction), and Auger spectroscopy. The experimental data are complemented by ab initio calculations, which allow for modeling of the absorption mechanism on a molecular level.

## 2. Experimental Section

The ESR measurements were performed in a specially designed ultrahigh vacuum ESR chamber which has been described in detail previously,<sup>18</sup> as well as the special sample design and the use of a liquid-helium cryostat, which allowed cooling of the crystal to 40 K. The electronic part of the ESR spectrometer (Bruker B-ER 420) has been improved by building in a new X-band microwave bridge (Bruker ECS 041 XK) and lock-in amplifier (Bruker ER 023 M). This modification led to a clear increase of the signal-to-noise ratio. The ESR ultrahigh vacuum chamber was equipped with a quadrupole mass spectrometer that allowed for the registration of multimass TPD spectra.

The NEXAFS spectra were taken at the synchrotron in Berlin (Berliner Elektronenspeicherring-Gesellschaft für Synchrotronstrahlung mbH, BESSY) using the HE-TGM2 monochromator. The ultrahigh vacuum chamber has been described elsewhere.<sup>19</sup>

\* Present address: Fritz-Haber-Institut der Max-Planck-Gesellschaft, Faradayweg 4–6, 14195 Berlin, Germany.

<sup>†</sup> Dedicated to Professor Georg Hohlneicher on the occasion of his 60th birthday.

<sup>⊗</sup> Abstract published in *Advance ACS Abstracts*, December 15, 1996.

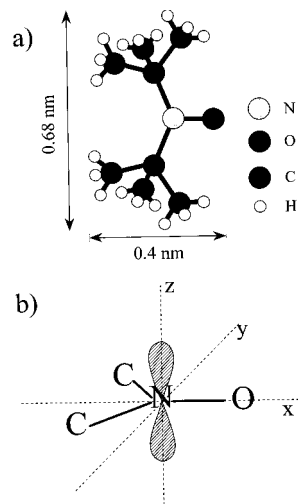


**Figure 1.** (a) Structure and magnitude of the DTBN molecule. (b) Standard coordinate system for the nitroxide group.

The XPS spectra were measured in a MXPS chamber which is described in ref 20. All ultrahigh vacuum chambers have base pressures in the range of  $1 \times 10^{-10}$  mbar or better and are equipped with LEED/Auger units for substrate characterization and quadrupole mass spectrometers to perform at least single mass TPD measurements.

The  $\gamma$ -Al<sub>2</sub>O<sub>3</sub>(111) film was prepared on a NiAl(110) single crystal (orientational deviation <1%) according to a recipe by Jäger et al.<sup>21</sup> After the substrate was cleaned (sputtering with Ar ions followed by heating the crystal to 1000 °C), the crystal was oxidized and completely covered with a well-ordered oxide film. The oxide film coverage was checked with CO titration.<sup>22</sup> This oxide layer has been studied thoroughly with electron spectroscopic methods, LEED,<sup>21</sup> and scanning tunneling microscopy.<sup>23</sup> It shows a long-range order with a structure based on slightly distorted hexagonal oxygen layers with a packing of aluminum ions like in  $\gamma$ -alumina. The thickness of the oxide film is only about 0.5 nm. The adsorption of small molecules on this film has also been studied.<sup>24</sup>

DTBN was purchased commercially (Lancaster), carefully degassed, and used without further purification. It was stored in glass or Teflon-containers which were attached to dosing valves leading into the ultrahigh vacuum chambers. Before dosing, the DTBN flask was warmed to approximately 50 °C to increase the vapor pressure. The chamber atmosphere was then flooded with DTBN. The exposure are given in langmuirs  $\equiv$  Torr·s.

The program for simulating and fitting the experimental spectra was written by Beckendorf,<sup>25</sup> and the part concerning molecular motion was based on a program package developed by Freed and co-workers,<sup>26</sup> which utilizes the solution of the stochastic Liouville equation for the description of dynamic processes.<sup>27</sup>

### 3. Experimental Results

**(a) Thermal Programmed Desorption and Low-Energy Electron Diffraction.** Figure 2 shows TPD spectra from dosages between 1 and 10 langmuirs DTBN at an adsorption temperature of 100 K. Since the quadrupole mass filter has a low transmission for high masses, it was not possible to detect the molecular ion with  $m/e = 144$  in the monolayer regime. The signals with the highest intensity in the cracking pattern of DTBN (using an ionization energy of 70 eV) with  $m/e = 39$  (C<sub>3</sub>H<sub>3</sub><sup>+</sup>) and 41 (CH<sub>3</sub>CN<sup>+</sup>, not shown here) can be used instead to follow the desorption from the surface as the multimass data

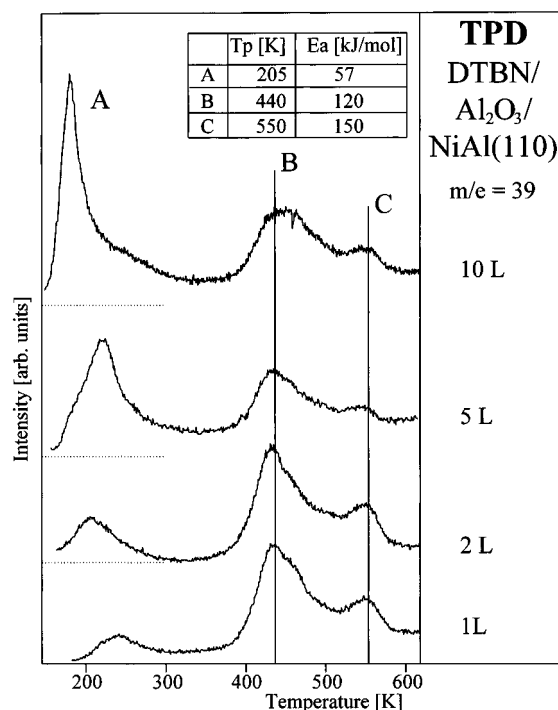


**Figure 2.** Thermal programmed desorption spectra of DTBN/Al<sub>2</sub>O<sub>3</sub>-NiAl(111). The intensity of the fragment with  $m/e = 39$  is shown. One feature from multilayer desorption (A) and two monolayer desorption states (B and C) can be seen. The desorption energies are also given.

revealed. A discussion of the cracking pattern has been given by Kostyanovskii and Khafizov.<sup>28</sup>

The TPD spectra in Figure 2 show three features marked A, B, and C. The intensity of peak A at a desorption temperature around 200 K increases with the DTBN dose. No saturation of this desorption state could be obtained. It is therefore identified with the desorption of the DTBN multilayer. The desorption energy is estimated by the Redhead formula<sup>29</sup> to be 57 kJ/mol; this value is probably dominated by van der Waals interactions in the multilayer.

The two features at higher temperatures, B around 440 K and C around 550 K, seem to be nearly fully saturated after a dose of 1 langmuir. They are assigned to two adsorption states of DTBN in the monolayer regime. The desorption energies are 120 and 150 kJ/mol, respectively. These values suggest a strong chemisorption of the DTBN molecules of the alumina surface, a result which is different from the findings for a number of small molecules, e.g., CO, NO, and CO<sub>2</sub>,<sup>24</sup> which all desorb at temperatures well below 200 K from this surface.

The strong interaction between substrate and adsorbate also causes irreversible damage in the structure of the substrate visible after an adsorption/desorption cycle: The sharp and complex LEED pattern of the freshly prepared oxide<sup>21</sup> shows an increasing background after one cycle, while the numerous reflexes merge into six hexagonally arranged patches. If more cycles are completed, the single reflexes vanish completely into the six broad patches. So there is a loss of long-range order at the surface, but short-range order still survives. Some additional hints exist that this restructuring also increases the roughness of the surface. Unfortunately the LEED pattern could not be probed while DTBN is adsorbed on the surface, because the molecules decompose under irradiation with electrons.

**(b) XPS.** Figure 3 shows XPS spectra of DTBN on the Al<sub>2</sub>O<sub>3</sub> surface. In the upper panel, N 1s spectra are plotted. The signal-to-noise ratio is rather poor, although prolonged data accumulation times have been applied. After adsorption of 10 langmuirs of DTBN at 100 K, a relative strong peak at a binding

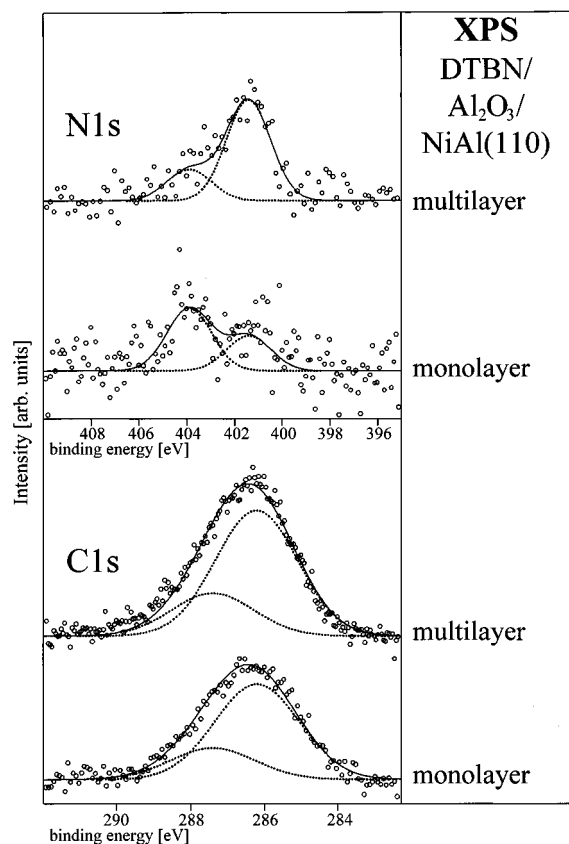


**Figure 3.** XPS spectra from the N 1s and C 1s photoemission of DTBN/ $\text{Al}_2\text{O}_3$ (111). The data are shown in a comparison of multi- and monolayer spectra. The fits are discussed in the text.

energy of 401.4 eV with a shoulder at 403.9 eV can be seen. The fit shows decomposition into two lines, which are attributed to the DTBN monolayer (higher binding energy) and multilayer (lower binding energy). This is supported by the fact that the peak at 401.4 eV is the only one remaining when the coverage is drastically increased.

For the second spectrum, the sample was warmed up to 300 K to desorb the multilayer. The peak at 403.9 eV is now more clearly visible, but some intensity also seems to remain at the position of the multilayer peak. Two facts should be emphasized: Firstly, the difference in binding energies between the predominant monolayer species and the multilayer is quite large (2.5 eV), so the nitrogen atom must be involved in binding to the surface. The shift to higher binding energies indicates a removal of electron density from the nitrogen atom. Secondly, the intensity remaining at 300 K at the peak position of the multilayer is a reference to a second DTBN species in the monolayer, which has already been seen in the TPD data in Figure 2. The electron density at the nitrogen atom of this second species would even correspond to those in an undisturbed molecule.

The remaining XPS data (C 1s, O 1s) give no further evidence about the nature of the bonding mechanism: The two spectra on the bottom of Figure 3 shows the C 1s emission in the mono- and multilayer. The decomposition shown is in accord with the existence of methyl and butyl carbon atoms with relative intensities of 3:1. No shifts in binding energies can be found between the spectra. The carbon atoms are therefore not involved in bonding the molecule to the surface. The O 1s spectra are comparable in intensity to the N 1s spectra in the monolayer regime but suffer from the large background signal due to the oxygen in the aluminum oxide, which could not be well separated.

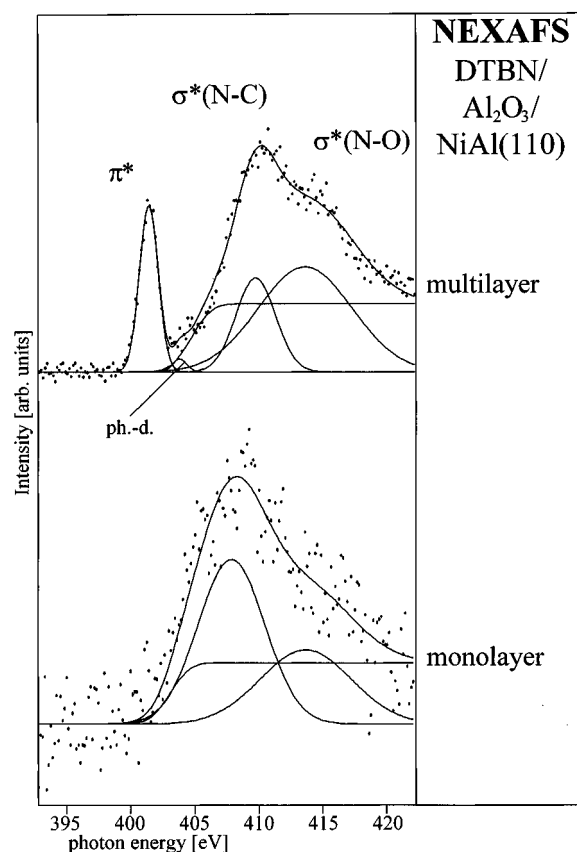


**Figure 4.** NEXAFS spectra from the N edge of DTBN/ $\text{Al}_2\text{O}_3$ (111) in a comparison of multi- and monolayers. The resonances and the fit are described in the text.

**(c) NEXAFS.** NEXAFS spectra were measured at the C, O, and N edges. At the C edge, a sharp, mixed valence/Rydberg  $\sigma^*(\text{C}-\text{H})$  resonance at 289.5 eV can be found as well as a broad  $\sigma^*(\text{C}-\text{C})$  resonance at 295 eV. When the coverage is decreased from the multilayer to monolayer regime, the resonances show no variation of either resonance positions or line shapes. This confirms that these groups play no important role in binding to the surface. A variation of the intensity as a function of the photon incidence angle has not been detected for both multi- and monolayer coverages. The spectra at the O edge suffer, like the O 1s XPS data, from the large background signal of the oxygen in the aluminum oxide. At high coverages, a  $\pi^*$  resonance at 533.1 eV and a  $\sigma^*$  resonance at 540.7 eV can be found. Lowering the coverage induces small shifts in the resonance positions ( $\pi^*$  to 532.1 eV,  $\sigma^*$  to 541.3 eV), but it was not possible to separate the DTBN signals from the background signal in the monolayer regime.

A comparison of the NEXAFS spectra taken at the N edge from multi- and monolayer coverages is shown in Figure 4. In the multilayer spectrum, the main features are marked: A sharp  $\pi^*$  resonance at 401.4 eV and two broader  $\sigma^*$  resonances, the  $\sigma^*(\text{N}-\text{C})$  resonance at 409.7 eV, and the  $\sigma^*(\text{N}-\text{O})$  resonance at 413.6 eV. A step function is added with respect to the increasing background due to photoionization at the absorption edge. An additional feature can be seen as a small shoulder (marked ph.-d.) at 404 eV. The intensity of this peak increases with increasing measuring time, so it is attributed to a photo-decomposition product of DTBN. No preferred orientation of the DTBN molecules can be found by varying the incidence angle of the incoming photons in the multilayer regime.

In the NEXAFS spectrum of a monolayer preparation at the bottom of Figure 4, the most remarkable feature is the complete absence of the  $\pi^*$  resonance. The  $\sigma^*(\text{N}-\text{C})$  resonance only

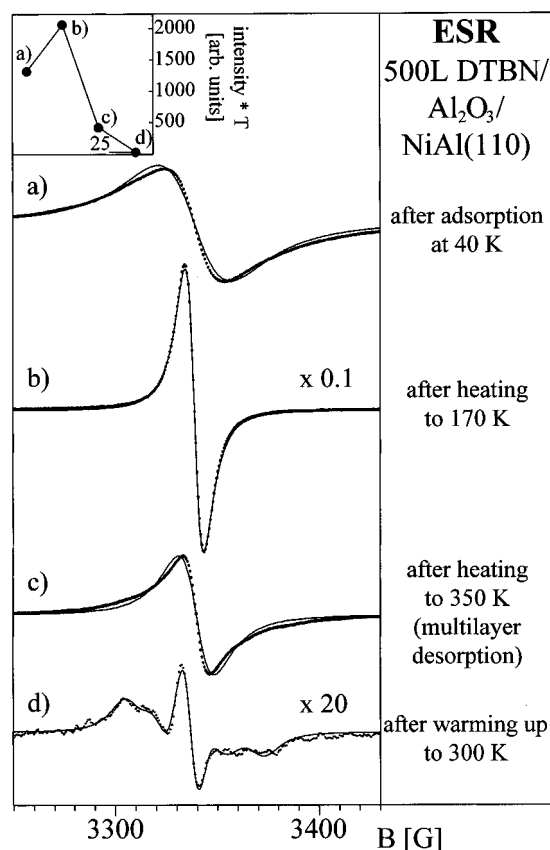


**Figure 5.** ESR spectra of DTBN/Al<sub>2</sub>O<sub>3</sub>(111). The changes going from multi- to monolayer coverages (a–c) are shown. The effect of an equilibrium in the monolayer (c, d) is also presented. The inset displays the course of the integral intensities of the spectra.

shows a small shift to lower photon energies. The absence of the  $\pi^*$  resonance may have several causes, e.g., extensive broadening through lifetime shortening and an interaction of the  $\pi^*$  orbital with the substrate or photodecomposition of the molecule, although no resonance of a photodecomposition product can be seen. Because the half-filled  $\pi^*$  orbital is also responsible for the paramagnetism of the DTBN molecule, the ESR data will be helpful to interpret the  $\pi^*$ -resonance attenuation.

An evaluation of the relative intensities of the  $\sigma^*(\text{N}-\text{C})$  and the  $\sigma^*(\text{N}-\text{O})$  resonances for different incidence angles of the photon beam reveals a preferential orientation for the DTBN molecules in the monolayer: The molecules are arranged with an angle of about 70° between the N–O axis (molecular  $x$  axis; see Figure 1b) and the surface normal. Therefore, the molecules adsorb in-plane, the N–O group being parallel to the surface.

**(d) ESR.** The missing  $\pi^*$  resonance in the NEXAFS spectra of the monolayer regime suggests that the interaction of the molecule with the substrate has a drastic influence on the  $\pi^*$  orbital. Nevertheless, ESR spectra can be obtained for monolayer coverages of DTBN on the Al<sub>2</sub>O<sub>3</sub> film as well as from the multilayers: Figure 5 shows the changes in the ESR spectra going from multi- to monolayer coverages. After an exposure of 500 langmuirs of DTBN to the crystal surface at a temperature of 40 K, the ESR spectrum in Figure 5a was obtained: A broad, single line is observed due to the formation of a DTBN multilayer. The collapse of the hyperfine structure into a single line is caused by the so-called exchange narrowing.<sup>30</sup> The effect of increasing exchange can be seen in Figure 5b: This ESR spectrum has been measured after heating the multilayer to 170 K, just below its desorption temperature, and cooling to 40 K again. The line width has decreased and the fitted Lorentzian

approaches the line shape better than in Figure 5a. The heating procedure has activated the molecular mobility (rotations, diffusion) in the multilayer, and the molecules, which may just have stuck at an adsorption temperature of 40 K, approach a more ordered structure. This causes a greater overlap of the unpaired electrons wave functions, which leads to an increase of the exchange frequency.

The next experimental step was desorption of the multilayer by heating the crystal to 350 K. The desorption was monitored with the quadrupole mass spectrometer. After cooling to 40 K, the heating procedure was repeated once more to minimize readsorption. The ESR spectrum taken afterwards is shown in Figure 5c: The signal has lost intensity and broadened again, and the fitted Lorentzian line matches the experimental spectrum even less perfectly. The reason is a decrease of the exchange frequency: The three-dimensional (3D) DTBN clusters, forming the multilayer, have reduced to a two-dimensional (2D) film covering the surface. But it turned out that the closed 2D array of ESR-active molecules is a metastable form of the monolayer: The helium flux of the cryostat was stopped, and the crystal was allowed to warm to 300 K within several hours. Afterwards, a resolved ESR spectrum, which is now governed by spatial anisotropy and hyperfine interactions, was measured (see Figure 5d). The spectrum has lost further intensity indicated by the decrease of the signal-to-noise ratio. The insert in Figure 5 shows the course of the integral intensities of the ESR signals. The expected Curie behavior of a paramagnetic molecule has been filtered out by multiplying the intensities with the measuring temperatures. (The first increase of the ESR intensity after heating the multilayer to 170 K has not been clarified fully up to now. It is possible that the abrupt freezing process at 40 K produces a metastable form of DTBN agglomerates in the multilayer, which decay under heating.)

The loss of intensity between the spectra in Figure 5c and 5d as well as the loss of intermolecular interactions (no exchange interactions) indicates that both the number and the concentration of the ESR-active molecules have decreased. One possibility is desorption of DTBN molecules from the surface. This is unlikely for several reasons: Firstly, the temperature of 300 K is well below the desorption temperatures of the monolayer states, and the crystal has already been heated to 350 K. Secondly, the ESR spectrum in its last form is stable for more than a day without any further loss of intensity. Thirdly, the TPD spectra of preparations held at 40 K or warmed to 300 K show the same intensities for the monolayer desorptions. It is more reasonable that a part of the molecules have been converted into a second, nonparamagnetic adsorption state. These DTBN molecules are still present on the surface but do not show an ESR spectrum and do not interact with the still ESR-active molecules.

The spectrum of Figure 5d has been fitted with a distribution of DTBN molecules in motion. The simulation includes a model for the molecular dynamics. This latter aspect is the subject of a further publication.<sup>31</sup> To separate the information contained in the spectrum from motional effects, the crystal was again cooled to 40 K to freeze out the molecular motion. Afterwards, the uppermost spectrum in Figure 6 has been obtained. The important facts here are the magnitude of the hyperfine splitting and the missing of an angular dependence of the spectra.

The separation of the outer extrema in the uppermost spectrum in Figure 6, marked 2A<sub>zz</sub>, the largest component of the  $A$  tensor,<sup>17</sup> is sensitive to a spin-density redistribution in the molecule, which may depend on an interaction with its chemical surroundings.<sup>32</sup> In a matrix of relatively weak interacting molecules such as tetramethyl-1,3-cyclobutandion,

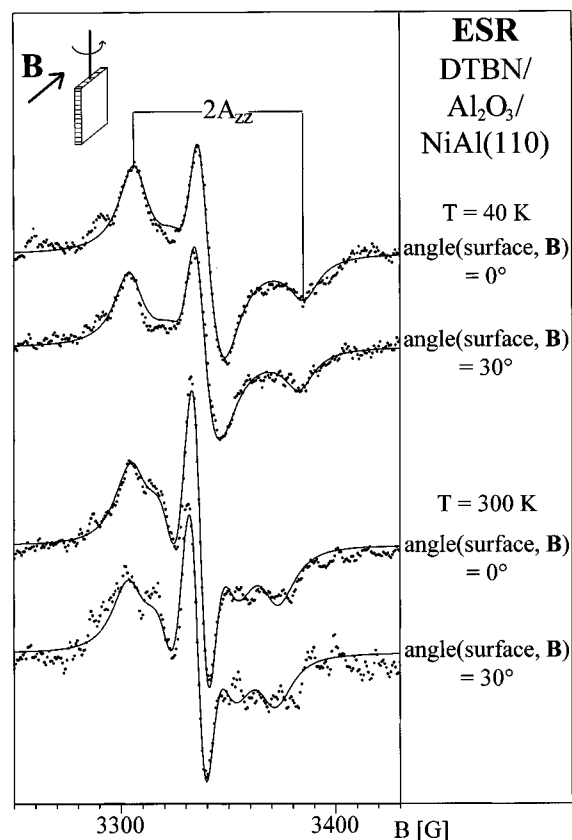


**Figure 6.** Angular dependence of the monolayer ESR spectra of DTBN/ $\text{Al}_2\text{O}_3$ (111). The experiment was done at 40 (two uppermost spectra) and 300 K (two lowermost spectra). The sketch illustrates the turning angle.

$A_{zz}$  takes the value of 31.78 G,<sup>17</sup> in a matrix of DTBN molecules 35.5 G,<sup>33</sup> and in the strong complex with  $\text{AlCl}_3$  47.0 G.<sup>34</sup> Another cause for a variation in the hyperfine interaction may be a bending of the molecular frame.<sup>35</sup> In the present case,  $A_{zz}$  has a value of 38.5 G. This finding is important with respect to the former adsorption model<sup>36</sup> and is discussed below.

The fit for the uppermost spectrum in Figure 6 was simulated using a 3D random distribution of static molecules. To demonstrate the absence of orientational effects, the crystal surface (normally lying in the direction of the magnetic field  $\mathbf{B}$ ; see sketch in Figure 6) was turned about an angle of  $30^\circ$  and the second spectrum in Figure 6 was measured. No significant changes can be found between the spectra, as one would expect for nonoriented molecules. Simulations show that just a fraction of 30% oriented molecules should lead to significant line-shape changes. The two lowermost spectra in Figure 6 show the results of the same experiment at a crystal temperature of 300 K. Between these two spectra, no significant difference can be found. The changes in line shape from 40 to 300 K are based on the thermal activation of molecular motion. The absence of a preferred orientation seems to be in contradiction to the NEXAFS results, which reveal a strongly inclined adsorption geometry for the DTBN molecules. This point will be clarified in the discussion of the adsorption model for this system (see below).

Figure 6 also shows that the spectra at 40 and 300 K are of comparable intensity. The susceptibility of a paramagnetic molecule should obey Curie's law, which, however, predicts a strong decrease ( $-86\%$ ) for the ESR intensity at 300 K. So the temperature dependence of the intensity has been studied: Figure 7 shows the ESR intensity of the full DTBN monolayers. The intensities have again been Curie-corrected (multiplication

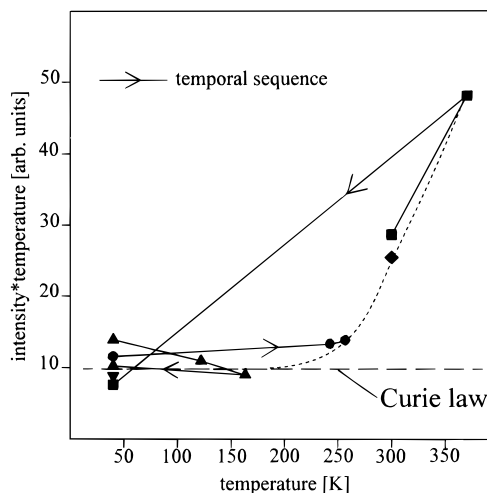


**Figure 7.** Temperature dependence of the integral ESR intensity of monolayer preparations in a Curie-corrected representation. Different symbols represent different preparations. The arrows indicate the sequence of measurements. The dashed horizontal line corresponds to pure Curie paramagnetism.

of the integral intensities with the measuring temperatures) and cover the full temperature range (40–370 K) accessible. All coverages have been prepared by thermal treatment of multilayers adsorbed at 40 K. Different symbols represent different monolayer preparations. The arrows indicate the sequence of measurements regarding the same preparation. The dashed horizontal line shows the behavior of a pure Curie paramagnet in this representation.

Up to temperatures of 200–250 K, the Curie law is obeyed, but at higher temperatures, an unusual increase of the intensity can be found. The course of the experiment covering the full temperature range ( $\blacksquare$ ) shows that this effect is reversible in contrast to the strong intensity loss that accompanies the first heating cycle of the monolayer (Figure 5c and 5d). It is likely that the two adsorption states establish a balance above 200 K. Below this temperature, an exchange between the states is frozen out and the number of molecules in the ESR-active state is constant. Since the ESR-active state is more populated with increasing temperature, its binding energy must be lower than that of the inactive state. It has to be mentioned that at 370 K, the fraction of ESR-active molecules is still well below 10% of the full monolayer.

Before discussing an adsorption model, one last observation has to be reported: All data presented before were measured after adsorption has taken place at low temperatures (40 K for the ESR measurements, 100 K for the other experiments). Since the desorption of the monolayer states occurs well above room temperature, an attempt was made to adsorb DTBN on the  $\text{Al}_2\text{O}_3$  surface at room temperature. This method would avoid a population of the multilayer state, but it leads to the population of a new, third adsorption state. Figure 8 shows the effects visible in the ESR spectrum obtained after an exposure of the surface to 4000 langmuirs of DTBN at room temperature. The dose has been chosen to saturate the monolayer. Two features appear in the spectrum: An additional broad signal underlies the structured ESR spectrum discussed before. Figure 8 also contains a decomposition into the two parts used for the simulation: For the simulation of the structured part, the same parameter set as in the simulation of the room-temperature spectra in Figure 5 and 6 has been used. The additional part is represented by just a single Lorentzian line. At the bottom of Figure 8, the difference between the experimental spectrum and the structured component of the simulation is shown. A

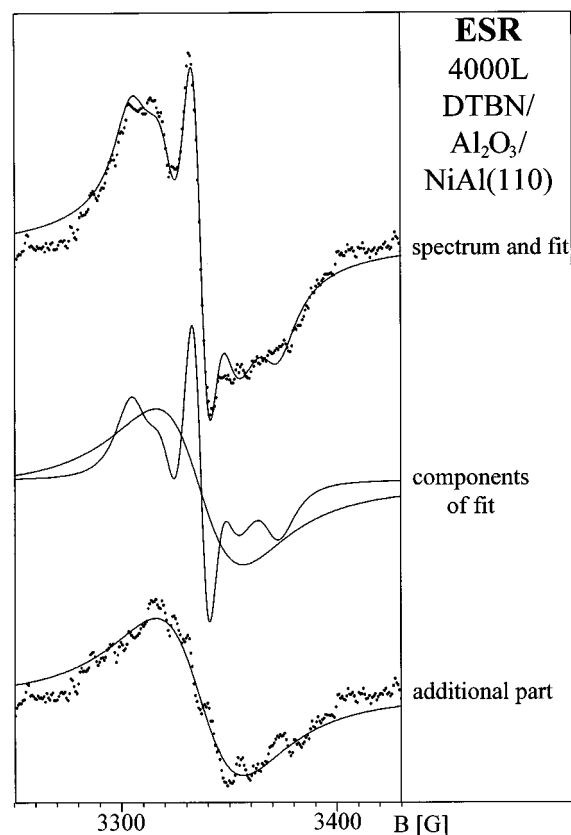


**Figure 8.** ESR spectrum of DTBN/Al<sub>2</sub>O<sub>3</sub>(111) adsorbed at room temperature (top). A decomposition of the simulation (middle) as well as the separated additional part in the spectrum (bottom) is also shown.

Lorentzian line fits the remaining broad resonance well in the center region but has too much intensity in the wing regions. So the observed signal has a more Gaussian profile, like an unresolved hyperfine splitting. Since the additional signal is quite structureless, no detailed information can be obtained. Warming the prepared layer to 370 K leads to complete loss of the broad feature, indicating that this state must be a metastable adsorption form. The molecules are probably converted into the ESR-inactive state, because no difference can be found in the TPD spectra of preparations made at 40 and 300 K.

#### 4. Discussion

The presented data reveal a quite complicated adsorption behavior for DTBN on the Al<sub>2</sub>O<sub>3</sub>/NiAl(110) surface. The ESR spectra indicate that three different forms of adsorbed DTBN exist, two ESR active and one inactive, which was confirmed indirectly via intensity measurements. The NEXAFS, XPS, and TPD data give more information about this non-ESR-active adsorption state. As XPS and NEXAFS data have shown, the NO group is responsible for binding the molecule to the surface. There are three possibilities for the binding mechanism: a bond via the oxygen atom or via the nitrogen atom or a mechanism involving both atoms. This approach would offer at least one binding mechanism for each adsorption form and will be discussed in detail in the following.

Since the oxygen atom of the DTBN molecule is more exposed than the nitrogen atom, the simplest case is a bonding via donation of a lone pair orbital of oxygen. An aluminum ion would be expected to be the acceptor center at the surface. Such an adsorption form of the DTBN molecules will be called from now on species I. This complexation changes the electronic structure of the DTBN molecules: Figure 9 shows two resonance structures representing the undisturbed N–O

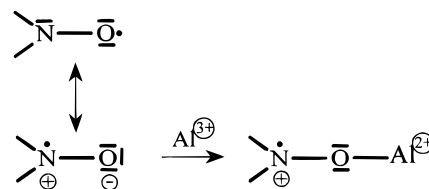


**Figure 9.** Effects of a complexation of the DTBN molecule in a valence picture.

group (left) and one for the complex (right). This picture is simple, but it also shows some important trends going from the isolated molecule to the complex: Firstly, the transfer of electron density induces a (partial) positive charge at the nitrogen atom. This charge redistribution can be responsible for the observed binding energy shift of the N 1s electrons from multilayer to monolayer coverages in the XPS data. Secondly, the unpaired electron survives in the complex and is now located (mostly) at the nitrogen atom. The ESR spectrum of such a complex should show an increase in the hyperfine interaction of the unpaired electron with the <sup>14</sup>N nucleus. This increase is seen in the experimental spectra in the change of  $A_{zz}$  from 35.5 G<sup>33</sup> in the multilayer to 38.5 G in the monolayer (see Figure 6).

The ESR spectrum of species I is indicative of complex dynamic behavior.<sup>31</sup> This may be a part of the explanation for the lack of orientational effects in the ESR spectra. Also, it cannot be necessarily assumed that the molecules freeze only in their equilibrium position at low temperatures. Additionally, the long-range order of substrate is lost through the strong interaction with the adsorbate. The orientation of different parts of the surface according to magnetic field **B** may also differ. The remaining orientational effects may be unresolved in the spectra, because the observed line widths are greater than 10 G (fwhm).

The inconsistency between the ESR and NEXAFS data concerning molecular orientation is caused by the fact that these methods see two different molecular species: The ESR experiment is exclusively sensitive to the ESR-active molecules of species I, while the NEXAFS experiment detects all molecules, but the ESR-inactive molecules of species II, discussed below, represent more than 90% of the monolayer population. Since the NEXAFS lines are relatively broad, the sensitivity is not high enough to detect the minorities of the  $\pi^*$  resonance.

The model of adsorption species I is compatible with a part of the obtained data, the ESR spectra as well the N 1s binding energy shift. A fundamental question, however, is still left out, namely, whether the binding energy of such a complex is large enough to explain the high binding energy found in the TPD experiment. Therefore, model calculations using the Gaussian-92 program package<sup>37</sup> have been performed to estimate the adsorption energy of the complex. The alumina surface was represented by an Al(OH)<sub>3</sub> cluster; the DTBN molecule has been replaced by a dimethyl nitroxide (DMN) molecule to reduce the computational effort but still leaves the important chemical ingredients in the problem. The calculations have been done on the restricted open-shell Hartree–Fock (ROHF) level as well as using Møller–Plesset perturbation theory up to the second order (MP2). Details of the calculation can be found elsewhere.<sup>38</sup> An energy minimum of 110 kJ/mol was found for an Al–O–N angle of 132° and a distance  $r(\text{Al–O})$  of 2.08 Å. There is fairly good agreement with the desorption energy of the low-temperature feature in the TPD spectra at 440 K (B in Figure 2), for which a binding energy of 120 kJ/mol was estimated. There should be some additional van der Waals forces between the CH groups of the molecule and the surface, which are not included in the model calculation and may account

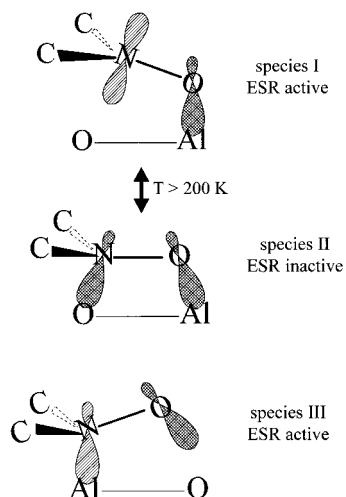


**Figure 10.** Adsorption model for DTBN/ $\text{Al}_2\text{O}_3(111)$ . The three adsorption species discussed in the text are illustrated. The exchange between species I and II is indicated. The Al–O distance in the surface corresponds to the sum of the ionic radii.

for the difference. These findings support the model for adsorption species I. An illustration of this adsorption form is given in Figure 10.

The second adsorption form, species II, must be ESR inactive, since the conversion into this form causes the loss of intensity shown in Figure 5c and 5d. A second effect concomitantly appearing with the loss of ESR activity is the attenuation of the  $\pi^*$  resonance seen in the NEXAFS spectra. Both can be explained by a direct interaction between the nitrogen atom and the surface. Since the desorption at 440 K (B in Figure 2) is attributed to species I, the desorption at 550 K (C in Figure 2) must be identified with species II. The higher binding energy of this desorption state indicates that the interaction of the molecule may be due to additive N–surface and O–surface interactions. A doubly bonded molecule would also explain the preferred orientation found in the NEXAFS data, because no motional effects can mimic a random distribution of molecular orientations. The in-plane adsorption geometry is in line with an interaction through both the nitrogen and oxygen atom with the surface.

The second bond probably involves a transfer of electron density from the surface to the nitrogen atom, because in the single-bond complex of species I, which is the precursor for the formation of species II, the nitrogen atom is (partly) charged positive. A filling up of the  $\pi^*$  orbital with electron density from an oxygen ion at the surface also forbids a further excitation of N 1s electrons into this orbital (strong attenuation of the  $\pi^*$  resonance) and destroys the radical character of the molecule (ESR inactivity).

The weak structure in the monolayer N 1s XPS spectra remaining unshifted at 401.4 eV (see Figure 3) should belong to species II. The electron transfer from the substrate compensates the positive charge at the nitrogen atom of species I, so the signal appears at the position of undistributed (multilayer) DTBN. A serious problem is the relative intensity of the two XPS signals: More than 90% of the DTBN molecules should be in the adsorption state described as species II at room temperature. So, naively, the intensity of the unshifted signal should be predominant, but the data show just the opposite. This could be due to several reasons. One possibility is that the distribution of the species is not uniform across the surface. Another is that the N 1s ionization of DTBN involves complex multielectron effects as has been discussed for NO-containing organic molecules which render a simple intensity/concentration

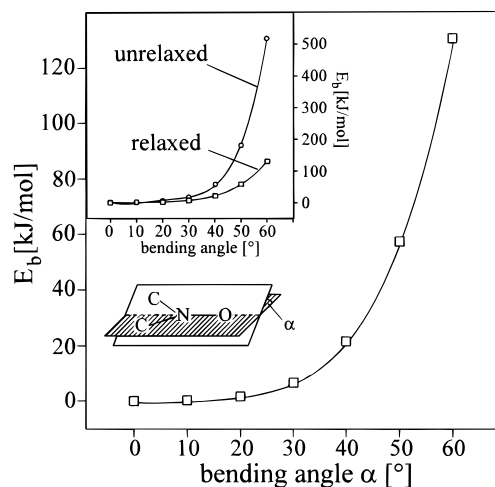


**Figure 11.** Effects of a bending of the molecular frame on the internal energy of the DTBN molecule obtained from ab initio calculations. The sketch illustrates the bending angle  $\alpha$ . The inset shows the influence of relaxation on the molecule's other structural parameter. See text for further explanation.

interrelation undetectable.<sup>39</sup> At present, that is not clear, but there is sufficient additional evidence for the presented adsorption model, so the intensity of the N 1s ionization is disregarded for the moment. A further argument for bonding between nitrogen and oxide oxygen is a geometric one: Since the oxygen atom of the molecule is connected with an aluminum center on the surface only, the six oxygen ions, arranged hexagonally around the aluminum ion, are available for bonding with the nitrogen atom.

Beside all positive arguments for an interaction between the nitrogen atom and the surface, the central question concerns the accessibility of the nitrogen atom. For effective bonding, the two *tert*-butyl groups shielding the nitrogen atom must be bent away. A model calculation, to quantify the interaction between both oxygen and nitrogen atoms with the alumina surface, is difficult: Firstly, the *tert*-butyl groups must be accounted for so that no smaller molecule can replace DTBN in this calculation. Secondly, a much bigger cluster representing the surface has to be used. The number of atoms involved in such a model is too large, to perform a high-quality ab initio calculation. Therefore, another attempt has been made to obtain a crude estimate: Calculations on the ROHF level (using a 6-31G\* basis set) have been performed to estimate the influence of a bending of the *tert*-butyl groups on the internal energy of the DTBN molecule.<sup>38</sup> Figure 11 shows the additional energy as a function of the bending angle  $\alpha$ . This angle is defined as the angle between the two planes containing nitrogen, oxygen, and one of the two tertiary carbon atoms, respectively (see sketch in Figure 11). This parameter has been fixed in the calculations; a relaxation of the other bonding angles and bond lengths has been allowed. For small bending angles, relaxation plays no important role, as the comparison of the energies of relaxed and unrelaxed structures shows (insert in Figure 11).

The energy needed is surprisingly low for small bending angles. Up to 40°, the internal energy is not raised higher than 20 kJ/mol. This energy increase can be balanced by the energy gain through a second bond to the substrate. However, the unknown parameter is still the energy gain from a  $\text{N}_{\text{DTBN}}-\text{O}_{\text{alumina}}$  bond. The bond energy may be estimated to be approximately the difference of the binding energies of the monolayer species plus the needed bending energy (approximately 20 kJ/mol). Since the desorption energies may still contain contributions due to activation barriers, the difference

in binding energies has been obtained from the ESR intensities: Assuming the existence of a temperature-dependent equilibrium constant and a Boltzmann distribution over the two adsorption species, a value for the energy difference can be calculated. The ESR intensities from Figure 7 have been taken to be proportional to the number of ESR-active DTBN molecules in the monolayer. The ESR intensity of the spectrum in Figure 5c is taken to be proportional to the whole number of molecules of a complete monolayer. These assumptions lead to an estimate for the energy difference of about 10 kJ/mol. Therefore, the binding energy of the second bond of species II should be on the order of 30 kJ/mol, which appears to be a reasonable value. Figure 10 shows a picture of species II.

For the third adsorption form, species III, there exists much less information, since its ESR spectrum is quite structureless. If the assignment for the bonding to the surface (via nitrogen, oxygen, or both) is correct for the first two species, the bonding via the nitrogen atom alone (see Figure 10) is left for this species. In fact, a bond of the nitrogen atom to an aluminum center on the surface would explain the change in the structure of the ESR spectrum: The <sup>27</sup>Al nucleus (natural abundance 100%) has a nuclear spin  $I = 5/2$ ,<sup>40</sup> so the additional hyperfine interaction will cause an additional 6-fold splitting of each line in the ESR spectra. Such a type of spectrum with partly resolved splitting has been observed by Lozos and Hoffman,<sup>36</sup> who studied the adsorption of DTBN on polycrystalline  $\gamma$ -Al<sub>2</sub>O<sub>3</sub> with ESR spectroscopy. They found both ESR-active species I and III but after different preparation conditions: For polycrystalline samples activated at 110 °C, species I was observed exclusively. Samples heated to 500 °C prior to adsorption first showed a species I signal, which converted reversibly to a species III signal by heating to 80–100 °C. The initial intensity losses were attributed to decomposition of DTBN molecules at active sites, so no ESR-inactive absorption form, as species II, was discussed. The behavior of DTBN on the polycrystalline  $\gamma$ -alumina is different from its behavior on the thin alumina film reported here. Polycrystalline samples cannot be characterized in detail with respect to structure and stoichiometry, and they almost always contain OH groups at the surface. So the reasons for discrepancies cannot be evaluated here in detail. The two ESR-active adsorption forms are found in both studies, although in the present case, the resonance lines in the spectrum of species III are broadened to a considerable amount so that the complex hyperfine structure is not resolved. This may be a lifetime effect with respect to the conduction electrons nearby in the NiAl substrate.<sup>41</sup>

The serious difference exists between the interpretations of the observed ESR signals in this and in Lozos and Hoffman's study.<sup>36</sup> These authors, indeed, assign the ESR spectrum of species I to a DTBN molecule bound to an OH group on the alumina surface and the ESR spectrum of species III to a DTBN molecule bound via oxygen to an aluminum center at the surface. The attribution of the O–H-bound species is mainly based on the coincidence of the  $A_{zz}$  values in the type I spectrum on alumina (this work, 38.5 G; Lozos and Hoffman; 38.6 G) and in a phenolic solution of DTBN (38.3 G<sup>36</sup>). The results of the present study suggest that this is just a coincidence. There are no hints of the existence of OH groups on the freshly prepared  $\gamma$ -Al<sub>2</sub>O<sub>3</sub>(111) film used here. A formation of OH groups can only be detected after massive water adsorption or preparation of aluminum hydroxide via coadsorption of metallic aluminum and water.<sup>42</sup> To support the fact that OH groups do not participate in the binding mechanism on the alumina film, the binding energy of a complex between a water and a DTBN molecule was computed at the ROHF level (applying a 6-31+G\*

basis set). An energy of 15.4 kJ/mol has been determined for a linear O–H–O–N complex. Such a low binding energy cannot explain the high thermal stability of the adsorbate, which has also been reported for the polycrystalline samples.

## 5. Summary and Conclusions

Three different adsorption forms of DTBN on the Al<sub>2</sub>O<sub>3</sub>(111) surface have been discovered and attributed to different molecular species. Adsorption at 40 K leads to the complexation of a surface aluminum ion via a lone-pair orbital of the oxygen atom in the DTBN molecule. Thermal activation to room temperature starts a conversion of more than 90% of the adsorbed molecules into a second species, which shows an additional interaction between the nitrogen atom and a surface oxygen ion. Above 200 K, an equilibrium is established through dynamic exchange between both forms. Adsorption at room temperature leads to the population of a third adsorption form, which is identified with a DTBN molecule bound only with the nitrogen atom to an aluminum ion. These interpretations are confirmed by ab initio calculations on model systems.

The usefulness of ESR spectroscopy in surface science has been demonstrated in the present work on the complex system of DTBN adsorbed on Al<sub>2</sub>O<sub>3</sub>(111)/NiAl(110).

**Acknowledgment.** We are grateful to the Deutsche Forschungsgemeinschaft, the Ministerium für Wissenschaft und Forschung des Landes Nordrhein-Westfalen, the Bundesministerium für Bildung und Forschung, and the Fonds der Chemischen Industrie for financial support. T. Risse and T. Klüner thank the Studienstiftung des Deutschen Volkes for financial support. T. Klüner is also grateful to the Rechenzentrum der Ruhr-Universität Bochum for providing the computational facilities necessary for the theoretical investigations.

## References and Notes

- (1) Surface Science—The first thirty years. *Surf. Sci.* **1994**, 299/300.
- (2) Hüfner, S. *Photoelectron Spectroscopy*; Springer Series in Solid-State Science 82; Springer-Verlag: Berlin, Heidelberg, 1995.
- (3) Freund, H.-J., Umbach, E., Eds. *Adsorption on Ordered Surfaces of Ionic Solids and Thin Films*; Springer Series in Surface Science 33; Springer-Verlag: Berlin, Heidelberg, 1993.
- (4) Hofmann, F.; Toennies, J. P. *Chem. Rev.* **1996**, 96, 1307.
- (5) Haglund, R. F. *Chem. Rev.* **1988**, 88, 697.
- (6) Slichter, C. P. *Principles of Magnetic Resonance*, 3rd ed.; Springer Series in Solid-State Sciences; Springer Verlag: Berlin, 1990; Vol. 1.
- (7) Spiess, H. W. *Molecular Rotation and Nuclear Spin Relaxation*. In *Dynamic NMR Spectroscopy—NMR Basic Principles and Progress*; Diehl, P., Fluck, E., Kosfeld, R., Eds.; Springer Verlag: Berlin, Heidelberg, New York, 1978; Vol. 15.
- (8) Detje, M.; Röckelein, M.; Preyss, W.; Ebinger, H. D.; Jänsch, H. J.; Reich, H.; Veith, R.; Widdra, W.; Fick, D. *J. Vac. Sci. Technol. A* **1995**, 13 (5), 2532.
- (9) Wertz, J. E.; Bolton, J. R. *Electron Spin Resonance—Elementary Theory and Practical Applications*; Chapman and Hall: London, 1986.
- (10) Farle, M.; Zomack, M.; Baberschke, K. *Surf. Sci.* **1985**, 160, 205.
- (11) Schlienz, H.; Beckendorf, M.; Katter, U. J.; Risse, T.; Freund, H.-J. *Phys. Rev. Lett.* **1995**, 74 (5), 761.
- (12) Hoffmann, A. K.; Henderson, A. T. *J. Am. Chem. Soc.* **1961**, 83, 4671.
- (13) Wohlrab, S.; Winkelmann, F.; Kuhlbeck, H.; Freund, H.-J. *Springer Proc. Phys.*, in press.
- (14) Mestdagh, M. M.; Lozos, G. P.; Burwell, R. L., Jr. *J. Phys. Chem.* **1975**, 79, 1944.
- (15) Ekeinov, V. I.; Golubev, V. B.; Lunina, E. V.; Le-Viet-Fu; Selivanovskii, A. K. *Russ. J. Phys. Chem.* **1976**, 50 (3), 400.
- (16) Andersen, B.; Andersen, P. *Acta Chem. Scand.* **1966**, 20 (10), 2728.
- (17) Libertini, L. J.; Griffith, O. H. *J. Chem. Phys.* **1970**, 53 (4), 1359.
- (18) Katter, U. J.; Schlienz, H.; Beckendorf, M.; Freund, H.-J. *Ber. Bunsenges. Phys. Chem.* **1993**, 97, 340.
- (19) Cappus, D. Ph.D. Thesis, Ruhr-Universität Bochum, 1995.
- (20) Illing, G. Ph.D. Thesis, Ruhr-Universität Bochum, 1991.

- (21) Jäger, R. M.; Kuhlenbeck, H.; Freund, H.-J.; Wuttig, M.; Hoffmann, W.; Franchy, R.; Ibach, H. *Surf. Sci.* **1991**, *259*, 253.
- (22) Unpublished results: Desorption of CO from the NiAl(110) surface takes place around 300 K, from the oxide surface below 60 K. An adsorption/desorption experiment, therefore, gives evidence whether the oxide layer is closed or not.
- (23) Bertrams, Th. Diploma Thesis, Ruhr-Universität Bochum, 1993.
- (24) Jäger, R. M. Ph.D. Thesis, Ruhr-Universität Bochum, 1992.
- (25) Beckendorf, M. Ph.D. Thesis, Ruhr-Universität Bochum, 1995.
- (26) Schneider, D. J.; Freed, J. H. Calculating Slow Motional Magnetic Resonance Spectra: A User's Guide. In *Spin Labeling: Theory and Applications*; Berlinger, L. J., Reuben, J., Eds.; Plenum: New York, 1989.
- (27) Freed, J. H. Theory of Slow Tumbling ESR Spectra. In *Spin Labeling: Theory and Applications*; Berlinger, L. J., Ed.; Academic: New York, San Francisco, London, 1976.
- (28) Kostyanovskii, R. G.; Khafizov, Kh. *Dokl. Akad. Nauk SSSR* **1971**, *198* (2), 363.
- (29) Redhead, P. A. *Vacuum* **1961**, *12*, 203.
- (30) Mao, C. R.; Kreilick, R. W. *Chem. Phys. Lett.* **1975**, *34* (3), 447.
- (31) Katter, U. J.; Hill, T.; Risse, T.; Schlienz, H.; Beckendorf, M.; Klüner, T.; Hamann, H.; Freund, H.-J. To be published.
- (32) Cohen, A. H.; Hoffman, B. M. *J. Phys. Chem.* **1974**, *78*, 1313.
- (33) Unpublished results: The value was obtained from small DTBN aggregates in thin layers. The exchange rate was low enough so that the hyperfine structure was not completely averaged out.
- (34) Eames, T. B.; Hoffman, B. M. *J. Am. Chem. Soc.* **1971**, *93*, 3141.
- (35) Ellinger, Y.; Subra, R.; Rassat, A.; Douady, J.; Berthier, G. *J. Am. Chem. Soc.* **1975**, *97*, 476.
- (36) Lozos, G. P.; Hoffman, B. M. *J. Phys. Chem.* **1974**, *78*, 2110.
- (37) Frisch, M. J.; Trucks, G. W.; Head-Gordon, M.; Gill, P. M. W.; Wang, M. W.; Foresman, J. B.; Johnson, B. G.; Schelgel, H. B.; Robb, M. A.; Replogle, E. S.; Gomperts, R.; Andres, J. L.; Raghavachari, K.; Binkley, J. S.; Gonzales, C.; Martin, R. L.; Fox, D. J.; DeFrees, D. J.; Baker, J.; Stewart, J. J. P.; Pople, J. A. *Program Package "gaussian 92"*, Revision A; Gaussian, Inc.: Pittsburgh, PA, 1992.
- (38) Klüner, T.; et al. To be published.
- (39) Sjörgen, B.; Freund, H.-J.; Salaneck, W. R.; Bigelow, R. W. *Chem. Phys.* **1987**, *118*, 101.
- (40) Weltner, W., Jr. *Magnetic Atoms and Molecules*; Dover: 1983.
- (41) Korringa, J. *Phys.* **1959**, *16* (7-8), 601.
- (42) Libuda, J.; et al. To be published.